Predicting Failure in Glass—A General Crack Growth Model

M. Overend[1]; G. A. R. Parke[2]; and D. Buhagiar[3]

Abstract: The successful design of glass as a structural element depends mainly on the ability to predict failure with accuracy and ease. Over the last 30 years various failure prediction models have been put forward for determining the load bearing capacity of glass, some of which have been adopted in national codes of practice. The differences between these models translate into a wide range of glass strength and glass thickness values in glass design. This paper compares the mathematical formulations of a number of existing failure prediction models, and the differences between these models are identified and discussed. From these comparisons a general crack growth model (GCGM) based on established statistical failure theory with linear elastic fracture mechanics is proposed. The performance of the existing models and the proposed GCGM is compared by physical and numerical investigations. The proposed model is shown to provide a basis for an accurate and automated method for determining the tensile strength of glass subjected to static loads and valid for any geometry and support condition.

DOI: XXXX

CE Database subject headings: Glass plates; Window glass; Finite element method; Fractures; Statistics; Cracking; Predictions.

Introduction

Glass structures have evolved from traditional curtain wall glazing, in which the glass is supported along two or four edges by a metal framework, to the current point-supported structural glass assemblies, where the glass plates are connected to each other and to a supporting structure by discrete clamped or bolted fixings usually located toward the corners of the glass panels. Point-supported glass facades are often top hung, i.e., the upper plate of glass carries the self-weight of the plate below; therefore the glass plates in top-hung structural glass facades are subjected to a combination of lateral wind loads and in-plane load. Furthermore, various glass elements are increasingly being used as load bearing elements in locations other than the façade, e.g., glass beams or fins, glass stairs, glass floors, glass balustrades, etc.

The lack of an accurate and user-friendly methodology for determining the strength of glass, particularly one that caters to the wide range of possible loading and support conditions, induces engineers to adopt large safety factors and expensive prototype testing. In addition, there is a lack of published research and test data on the performance of the more recent forms of structural glass assemblies.

Despite these shortcomings, a number of failure prediction models have been proposed over the last 30 years. These models were originally developed for laterally loaded rectangular glass plates; however they provide a valuable source of information on the factors that affect glass strength and the mechanics of glass failure. These failure models include the pioneering work of Brown (Brown 1974) and the seminal work of Beason and Morgan (Beason 1980; Beason and Morgan 1984) that form the basis of the United States and Canadian codes of practice (ASTM 1997; CAB/CGSB 1989). Two of the more recent models are: the model proposed by Sedlacek et al. (1995) that forms the basis of the European code of practice (CEN 1997); and the crack growth model put forward by Fischer-Crippps and Collins (1995). The common approach of all these models is that maximum stress oriented theories are unable to portray the strength of glass accurately and that an accurate determination of the strength of glass should be achieved by relating the probability of failure to the factors affecting Griffith flaw characteristics. This is widely accepted as the most accurate approach by the glass design community, however the complexity of these models makes them unattractive for manual computation.

This paper summarizes the basic mechanics of glass failure with respect to the various factors that affect glass strength and discusses how the above-mentioned failure models allow for these factors. A general failure prediction model based on established statistical failure theory and linear elastic fracture mechanics is also put forward in this paper. The proposed model, referred to as the general crack growth model (GCGM), extends the Fischer-Cripps and Collins (1995) model to account for variations in the maximum and minimum principle stresses on the surface of the glass and covers the use of heat strengthened and fully tempered glass. An automated approach is subsequently used to compare the predictions obtained from the existing and proposed failure models. Thee predictions are verified by experimental investigations carried out by both the writers and by independent experimental investigations (Abiassi 1981; Dalgliesh and Taylor 1990; Norville et al. 1991).

[1]Lecturer, School of the Built Environment, Univ. of Nottingham, Nottingham NG7 2RD, UK (corresponding author). E-mail: mauro.overend@nottingham.ac.uk

[2]Professor, Dept. of Civil Engineering, School of Engineering, Univ. of Surrey, Guildford, Surrey GU2 5XH, UK.

[3]Senior Lecturer, Dept. of Building & Civil Engineering, Univ. of Malta, Msida, Malta.

Note. Associate Editor: Satish Nagarajaiah. Discussion open until January 1, 2008. Separate discussions must be submitted for individual papers. To extend the closing date by one month, a written request must be filed with the ASCE Managing Editor. The manuscript for this paper was submitted for review and possible publication on October 31, 2003; approved on June 19, 2006. This paper is part of the ***Journal of Structural Engineering***, Vol. 133, No. 8, August 1, 2007. ©ASCE, ISSN 0733-9445/2007/8-1–XXXX/$25.00.

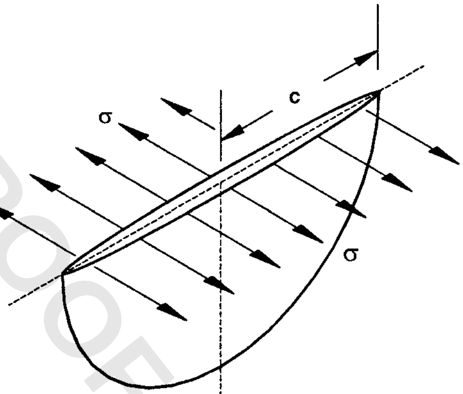

Fig. 1. Half penny crack (adapted from Lawn 1993)

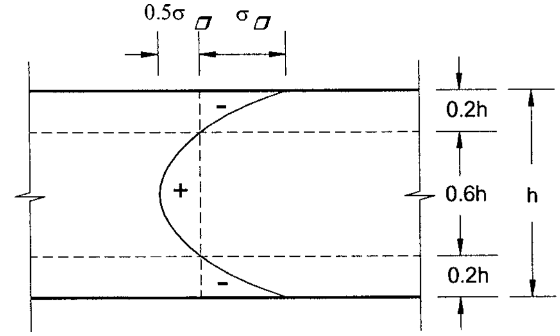

Fig. 2. Parabolic stress distribution resulting from tempering process (adapted from Laufs and Sedlacek 1999)

The Strength of Glass

The random molecular structure of glass lacks crystallinity or long-range order and has no slip planes or dislocations to allow yield before fracture; consequently, glass exhibits brittle fracture at a theoretical value between 15,000 and 21,000 MPa (Holloway 1973; Creyke et al. 1982). On freshly drawn glass fibers, tensile stresses of up to 5,000 MPa have been measured and, even when incorporated into a resin to form glass reinforced plastic, the glass fibers have a usable stress of 1,200 MPa (Sedlacek et al. 1995, Button and Pye 1993). However, the characteristic strength of architectural glass proposed by the draft European Standard is 45 MPa (CEN 1997) and weathered window glass was reported to fail at stress levels of around 25 MPa (Button and Pye 1993). Furthermore, the Institution of Structural Engineers (2000) proposed a value of 8 MPa for the design strength of annealed glass subjected to long-term stresses.

Mechanics of Glass Failure

These large variations between the theoretical and practical strength of glass were explained by A. A. Griffith in 1920 (Griffth 1920). Griffith argued that fracture did not start from a pristine surface, but from preexisting flaws (Griffith flaws) on that surface. Basing his work on the research carried out by Inglis (1913) on elliptical cavities in plates, Griffith went on to describe crack growth as a reversible thermodynamic process.

Irwin (Lawn 1993) extended the original Griffith energy balance concept to provide a means of characterizing a material in terms of its brittleness or fracture toughness. A convenient material property defined by Irwin is the stress intensity factor, K, which represents the elastic stress intensity near the crack tip and depends on the applied loading and the specimen geometry. The stress intensity factor for mode 1 loading is K_1, where mode 1 corresponds to normal separation of the crack walls under the action of tensile stresses and is given by

$$K_I = \sigma Y(\pi c)^{1/2} \tag{1}$$

where the shape correction factor, Y, accounts for different ratios of crack length to specimen width, and the proximity of the crack to the specimen boundaries. A value of 0.713 has been proposed for half-penny cracks in a semi-infinite glass specimen shown in Fig. 1 (Fischer-Cripps and Collins 1995; Lawn 1993). Irwin also described the resistance to fracture by means of the plane strain fracture toughness, K_{IC}, which is the critical value of the stress intensity factor in Eq. (1), i.e., when $K_I = K_{IC}$ instantaneous fracture occurs. A typical value for K_{IC} for soda lime glass is 0.78 $\mathrm{MPa}^{1/2}$ (Atkins and Mai 1988).

These fundamentals of fracture mechanics show that the tensile strength of glass is governed by the nature of the surface flaws and provide an explanation for the large scatter of results obtained when seemingly identical glass specimens are tested to failure. The presence of flaws on the glass surface also accounts for the fact that glass failure can usually be traced back to a single point of origin, known as the critical flaw, that rarely coincides with the point of maximum stress. This inherent variability associated with the surface flaw characteristics implies that the strength must be treated statistically and that maximum stress-oriented theory is unable to portray the tensile strength of glass accurately.

The most common way of reducing the deleterious effect of the flaws is by tempering the glass. In this process the glass is heated and then rapidly quenched, thus introducing a parabolic stress gradient within the thickness of the glass whereby the outside surface is stressed in compression (Fig. 2). Any externally applied force must overcome the surface precompression before any surface tensile stress can be set up. Tempered glass with a surface precompression of 120 $\mathrm{N/mm}^2$ is commercially available, however the presence of other surfaces such as at plate edges, corners, and holes may distort the parabolic stress distribution and consequently reduce the surface precompression at these locations (Laufs and Sedlacek 1999).

Flaw Statistics

The two-parameter Weibull distribution is reported to provide the best statistical representation of the strength of glass specimens (Weibull 1951; Behr et al. 1991). This distribution adopts two interdependent parameters m and k in order to predict the probability of failure P_f of a specimen given by Eq. (2)

$$P_f = 1 - \exp(-kA\sigma_s^m) \tag{2}$$

The surface strength parameters m and k can only be determined by experiment and form the basis of the existing failure models discussed in the ensuing section. From the various numerical and physical tests carried out (Beason 1980; Beason and Morgan 1984; Sedlacek et al. 1995; Dalgliesh and Taylor 1990; Norvelle et al. 1991, and Charles 1958), it may be concluded that the long-term strength of glass depends on the following parameters:

1. Duration of application of load.
2. Surface area of glass exposed to the tensile stress.
3. Orientations of the surface flaws with respect to the principle stresses on the surface of the glass.

Table 1. Surface Strength Parameters

Failure model	Surface strength parameters m	k
Brown (1974); Fischer-Cripps and Collins (1995) As-received glass	7.3	5.1×10^{-57} m^{-2} Pa$^{-7.3}$
Beason (1980) Weathered glass	6	7.19×10^{-45} m^{-2} Pa^{-6}
Beason and Morgan (1984) As-received glass	9	1.32×10^{-69} m^{-2} Pa^{-9}
ASTM (1997); CAN-CGSB (1989) Weathered glass	7	2.86×10^{-53} m^{-2} Pa^{-7}
Sedlacek et al. (1995); CEN/TC129/WG8 (CEN 1997) As-received glass	25	2.35×10^{-188} m^{-2} Pa^{-25}

4. Environmental conditions, especially humidity.
5. Magnitude and distribution of the net surface tensile stresses.

Existing Failure Models

The increasing use of glass as a load-bearing material has led to the development of a number of failure prediction models. The aim of these failure models is to arrive at a value of allowable load or stress for an acceptable probability of failure in terms of the environmental and geometrical parameters. The earliest such failure model, the *load duration theory*, was proposed by Brown in 1974 (Brown 1974). Beason (1980) and Beason and Morgan (1984) developed the *glass failure prediction model*, which constitutes the backbone of the United States (ASTM 1997) and Canadian (CAN/CGSB 1989) standards, and is based on the semiempirical thermodynamic formulations of Charles (1958). Recently an alternative treatment of the failure of brittle solids, derived from elastic fracture mechanics and subcritical crack growth, has emerged in the form of the crack growth models of Sedlacek et al. (1995) and Fischer-Cripps and Collins (1995). More recently, Porter and Houlsby (2001) have proposed an alternative design method with underlying fracture mechanics formulations similar to those adopted by Fischer-Cripps and Collins. These failure prediction models constitute a valuable source of information for the structural design of glass. However, these models have never been compared and therefore it seems opportune to do so.

The main discrepancies between the existing failure models arise from the adoption of dissimilar surface strength parameters m and k and from the different representations of the load duration, surface area, and flaw orientation effects on the tensile strength of glass. These aspects are discussed in detail in the following sequel.

The surface strength parameters shown in Table 1 and the probability distribution functions (PDFs) plotted in Fig. 3 reveal that there is good agreement between the functions adopted by Brown (1974), Fischer-Cripps and Collins (1995), ASTM (1997), and CAN/CGSB (1989). The Sedlacek et al. (1995) PDF, which forms the basis of the draft European Standard (CEN 1997), shows reasonable agreement with the Brown (1974), Fisher-Cripps & Collins (1995), ASTM (1997), and CAN/CGSB (1989) functions at low probabilities of failure. There is however a large disparity between the Sedlacek et al. (1995) model and the others at higher probabilities of failure. This is due to a high surface

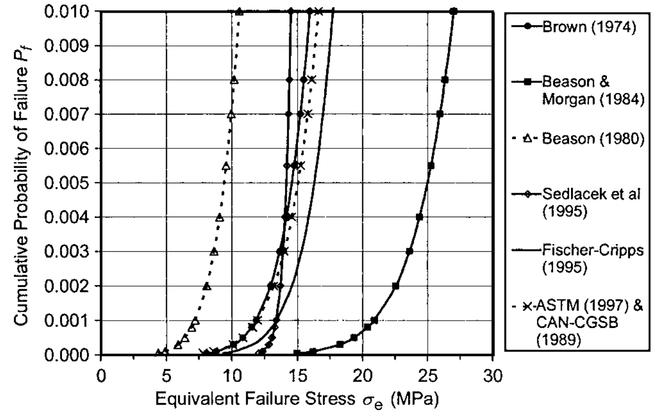

Fig. 3. PDF at low probabilities of failure (dotted lines represent weathered glass)

strength parameter ($m=25$) adopted by this model indicating an uncharacteristically low variability in glass strength. It is important to note that the Beason and Morgan (1984) PDF was derived from testing weathered glass and consequently provides the lowest strength values. The ASTM E-1300-97 (ASTM 1997) and CAN/CGSB 12.20-M89 (CAN/CSB 1989) functions were also formulated for weathered glass, however they provide a more optimistic strength prediction than Beason and Morgan (1984).

These differences in surface strength parameters result in considerable differences in the strength values of glass in practical applications. An example of this is shown in Table 2 in which the failure stresses have been derived for a 1 m^2 plate of annealed glass with a uniformly applied surface tensile stress and a 60 s load duration.

The existing models also account for degradation of the tensile strength of glass with increasing load duration. This phenomenon, termed stress corrosion (or static fatigue), is caused by the subcritical crack growth on the glass surface at stress levels below instantaneous failure stress. Under constant load and constant relative humidity, the 60 s equivalent stress may be expressed by

$$\sigma_e = \sigma_s \left(\frac{t_f}{60} \right)^{1/n} \tag{3}$$

where σ_s is derived from Eq. (2) and n=stress corrosion constant, the magnitude of which is dependent on environmental conditions, especially humidity.

The stress corrosion effects adopted by the various models, for a typical 1 m^2 uniformly stressed plate and a probability of failure

Table 2. Comparison of 1960s Equivalent Stresses

Failure model	1960s Equivalent failure stress (MPa) $P_f=1/125$	$P_f=1/1{,}000$
Brown (1974)	15.50	11.85
Beason (1980)	10.19	7.20
Beason and Morgan (1984)	26.24	20.89
ASTM (1997); CAN-CGSB (1989)	16.11	11.96
Sedlacek et al. (1995), CEN/TC129/WG8 (CEN 1997)	14.39	13.38
Fischer-Cripps and Collins (1995)	17.25	13.41

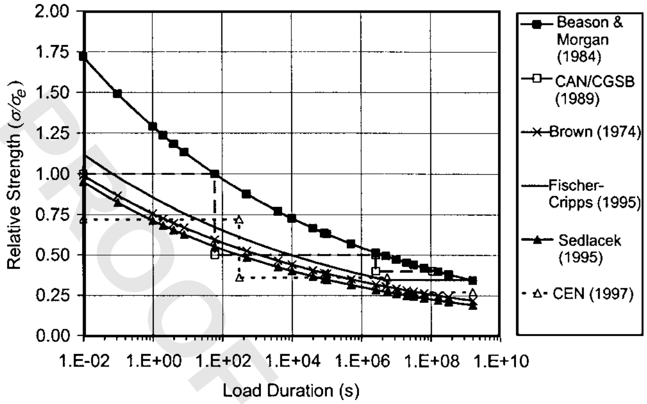

Fig. 4. Stress corrosion curves for annealed glass

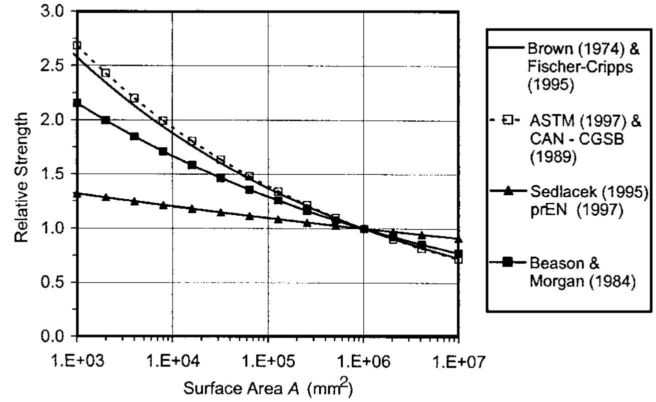

Fig. 5. Relative strength of annealed glass with variations in surface area (dotted lines represent weathered glass)

of 1/1,000, are shown in Fig. 4. The asymptotical ends to the Fisher-Cripps and Collins and the Sedlacek et al. load duration curves represent the static fatigue limits beyond which subcritical crack growth will not occur. The static fatigue limit shown on the Sedlacek et al. (1995) curve is that adopted by the draft European Standard (CEN 1997).

From Fig. 4, it is evident that the Beason and Morgan (1984) model provides the most optimistic prediction of glass strength. This is a direct result of the surface strength parameters adopted, as discussed in the previous section. However, the models represented by the continuous functions are in close agreement in terms of the relative strength of glass between long-term and short-term loads. For example, the tensile strength of glass subjected to a constant load for a 1-month duration ranges between 0.49 and 0.53 of the 60 s strength depending on the failure model adopted.

The CAN/CGSB (1989) step function provides a good lower-bound approximation to the Brown (1974) curve. The Fischer-Cripps and Collins (1995) and Sedlacek et al. (1995) load duration curves are in very close agreement. However there are two anomalies in the draft European Standard (CEN 1997). The first is that the step function set out by this standard straddles the Sedlacek et al. curve and therefore does not appear to provide a safe representation of the stress corrosion characteristics proposed by Sedlacek et al. (1995). Second, the static fatigue ratio of 27% adopted by the European standard is outside the 32–38% range of static fatigue limits reported elsewhere (Wan et al. 1961; Shand 1965; Wiederhorn and Bolz 1970; Wiederhorn 1977; Michalske 1983). In this latter case the European standard seems to overestimate the deleterious effects of stress corrosion.

The existing failure models also account for the reduction in the tensile strength of glass with increasing surface area. The relationships between the strength and the stressed surface are shown in Fig. 5. The relative strength on the ordinate Y axis represents the ratio of the tensile strength for a given surface area to the tensile strength of a 1 m^2 glass plate and equates to $(A_o/A)^{1/m}$.

Fig. 5 reveals that there is good agreement between the Fischer-Cripps and Collins (1995) curve, which is identical to Brown's relationship, and the ASTM (1997) and CAN/CGSB (1989) curves. There is less agreement between the above-mentioned curves and the relationship proposed by Beason and Morgan (1984), but the differences are within ±3% for a surface area between 0.5 and 4 m^2. The Sedlacek et al. (1995) strength versus area relationship implies that the surface area has a less pronounced effect on the strength of glass than that proposed by the other failure models. This discrepancy is mainly attributed to the relatively high surface strength parameter (m=25) adopted by the European standard.

Surprisingly, the crack growth models proposed by Fischer-Cripps and Collins (1995) and Sedlacek et al. (1995) fail to consider the effect of the orientation of the surface flaws and the magnitude of principle stresses on the tensile strength of glass. This is clearly a shortcoming, particularly because the propensity of a flaw to initiate failure (and hence the tensile strength) is a function of the orientation of the flaw with respect to the major and minor principal stresses σ_{max} and σ_{min}. (Fig. 6).

The variations of normal stresses with flaw orientations are included in the glass failure prediction model proposed by Beason (1980) which was subsequently extended by Beason and Morgan (1984). This was achieved by introducing a biaxial stress modification factor based on Weibull's formulation (Weibull 1951) such that Eq. (2) may be rewritten as

$$P_f = 1 - \exp[kA(c_b\sigma_s)^m] \qquad (4)$$

where

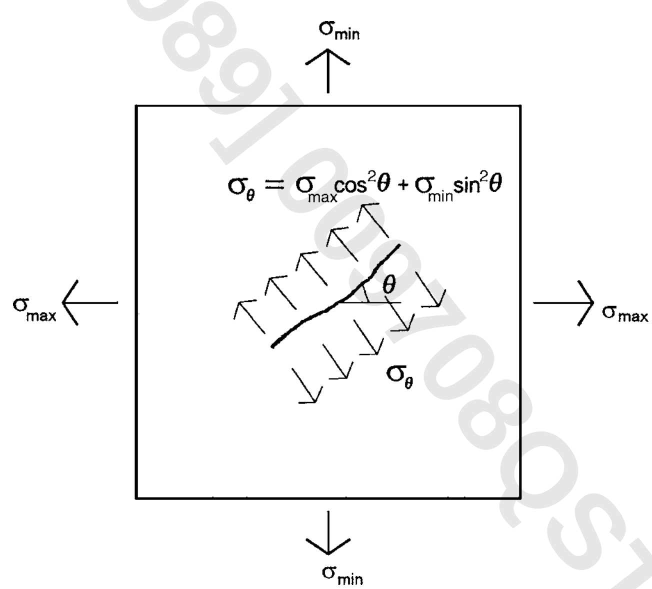

Fig. 6. Flaw orientation

$$c_b = \left[\frac{2}{\pi} \int_0^{\alpha} (\cos^2 \theta + n \sin^2 \theta)^m d\theta \right]^{1/m} \tag{5}$$

Formulation of General Crack Growth Model

From the comparisons carried out in the previous sections it is evident that the crack growth models are the closest representation of the failure mechanism at microscopic level, and are therefore, best suited to determine the probability of failure of glass. However, these models do not take into account all five factors listed in the previous section that are known to affect glass strength. Notably, the crack growth models proposed by Sedlacek et al. (1995) and Fischer-Cripps & Collins (1995) do not consider the effects of surface flaw orientation on the tensile strength of glass. From these two existing failure models the Fischer-Cripps and Collins model is preferred by the writers as it adopts a verified stress corrosion limit and surface strength parameters that are within the range of values reported elsewhere (Table 1).

Tensile Strength of Glass

Since tempered glass is used in the majority of structural glass applications it is therefore essential to account for the surface precompression in the proposed model. In tempered glass, the stress corrosion phenomenon only occurs after the applied tensile surface stress exceeds the residual precompression σ_r. Eq. (1) may therefore be used to characterize the instantaneous failure σ_s of glass with a modification, σ_r, to take into account the surface precompression induced by the tempering process as given by Eq. (6).

$$\sigma_s = [K_{IC}/Y(\pi c)^{1/2}] + \sigma_r \tag{6}$$

It is important to note that the thermally induced surface precompression is distorted close to free edges and holes in the glass (Laufs and Sedlacek 1999). Therefore the magnitude of σ_r depends on the location under consideration.

If the applied tensile stress exceeds the thermally induced surface precompression σ_r at a specific location, the net tensile stress may either cause a critical flaw to fail instantaneously or it may cause a flaw to grow subcritically, under sustained load, until it reaches a length that will cause failure of the glass. Since the static and pseudostatic load durations encountered in practice normally include medium and long-term loads ranging from a few minutes to the full service life, it is necessary to transform the instantaneous annealed glass failure strength, σ_s, to an equivalent (same probability) failure strength, σ_f, by taking into account the stress corrosion characteristics of glass. The σ_f/σ_p relationship, termed the stress corrosion modification factor k_{mod}, is equivalent to the ratio of stress concentration factors K_{IC}/K_I defined by Fischer-Cripps and Collins (1995), such that

$$K_I = \frac{K_{IC}\sigma_s}{\sigma_f} \tag{7}$$

The time required for a flaw to grow subcritically from its initial unstressed size to a final critical size that will cause failure was also derived by Fischer-Cripps and Collins (1995) and is given by

$$t_f = \frac{2K_I^{2-n}}{D(n-2)\sigma_s^2 Y^2 \pi} \tag{8}$$

by substituting Eq. (4) into Eq. (5) gives

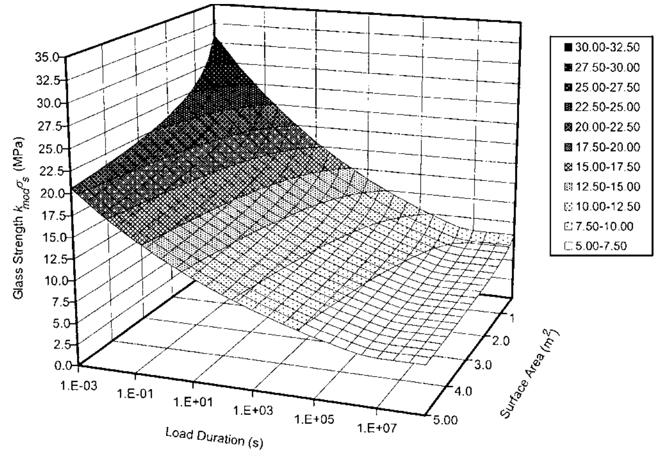

Fig. 7. Failure envelope for annealed glass

$$k_{\mathrm{mod}} = \frac{\sigma_f}{\sigma_s} = \left[\frac{t_f D(n-2) K_{IC}^{n-2} \sigma_s^2 Y^2 \pi}{2} \right]^{1/(n-2)} \geqslant 0.346 \tag{9}$$

where K_{IC} = critical stress intensity factor with a value of 0.78 $\times 10^6$ m$^{1/2}$ Pa (Atkins and Mai 1988), Y = shape correction factor with a value of 0.713 for half-penny cracks (Atkins and Mai 1988), n = static fatigue constant taken as 16, and σ_s = instantaneous stress applied for a time t_f. However, the stress corrosion modification factor, k_{mod}, is limited by a stress (or crack length) below which subcritical crack growth will not occur. This is represented by the 0.346 limit in Eq. (9).

The surface tensile strength σ_f may therefore be obtained from Eq. (10) as suggested in the Draft European Standard (CEN 1997):

$$\sigma_f = k_{\mathrm{mod}}\sigma_s + \sigma_r/\gamma_v \tag{10}$$

where k_{mod} = stress corrosion modification factor obtained from Eq. (9), σ_s = instantaneous failure stress for annealed glass obtained from Eq. (2) for a required probability of failure P_f, σ_r = surface precompression due to the tempering process provided by the manufacturer, and γ_v = safety factor depending on the surface precompression, the magnitude of which depends on the level of quality assurance. The draft European Standard (CEN 1997) uses the material safety factor, γ_v, to account for both the level of quality assurance and the reduced magnitude of precompression close to the edges of the glass. The values of γ_v suggested by the draft European Standard range between 1.5 and 2.4.

The combined influence of load duration and stressed area on the strength of glass may be expressed by means of a failure envelope for a given probability of failure (Fig. 7). The surface plotted in Fig. 7 represents the failure stresses for a range of load durations t_f and surface areas A, and a probability of failure P_f of 1/1,000. A glass specimen with a known surface area and load duration may be represented by a point in $P_f/A/t_f$ space. A point above the surface indicates that the probability of failure is greater than 1/1,000 and a point on or below the surface indicates that the glass specimen in question has a probability of failure that is equal to or less than 1/1,000, respectively. Interestingly, the plan view of this failure surface shown in Fig. 8 is very convenient for obtaining graphically the $k_{\mathrm{mod}}\sigma_s$ term used in Eq. (5).

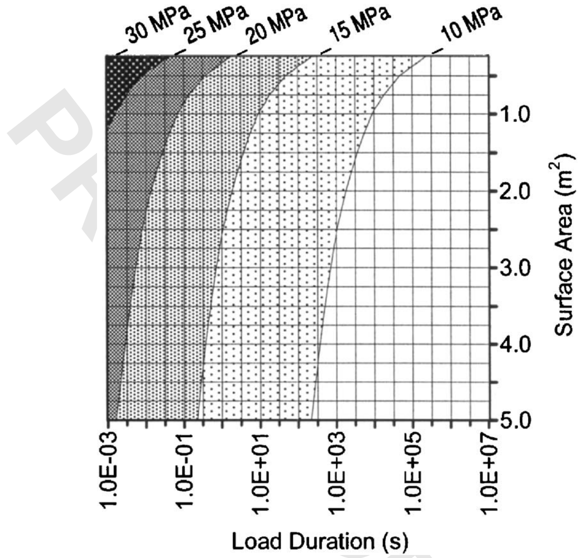

Fig. 8. Plan view of failure envelope

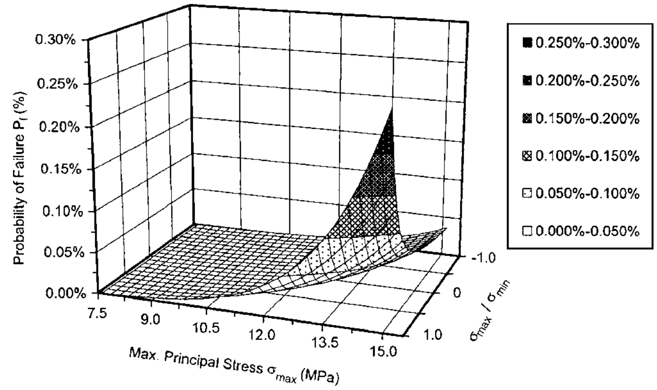

Fig. 9. Variations in probability of failure with nonuniform biaxial stresses

Applied Stress

The risk of failure experienced by a glass plate is related to the magnitude of the applied stresses which act normal to the longitudinal axis of the surface flaws as shown in Fig. 6. This is also known as mode I loading. The term σ_σ in Eqs. (2) and (9) are both derived from experiments where the stress is applied perpendicular to a crack (Wan et al. 1961; Shand 1965; Wiederhorn and Bolz 1970; Wiederhorn 1977; Michalske 1983). Although it is unlikely that the precise orientation of surface flaws on glass plates will ever be known, it is nevertheless possible to incorporate the variation of normal stress with flaw orientation as suggested by Beason and Morgan (1984) based on the formulations of Weibull (1951) as shown in Eqs. (4) and (5).

If the critical flaw is oriented at θ from the plane of the maximum principal stress $\sigma_{\max}$ and assuming that mode I loading is the only contributor to crack propagation, the stress applied perpendicular to a flaw shown in Fig. 6 may be rewritten as

$$\sigma_a = c_b \sigma_{\max} \tag{11}$$

where c_b=biaxial stress correction factor ranging from 0.77, for $\sigma_{\min}/\sigma_{\max}=1.0$, to unity, for $\sigma_{\min}/\sigma_{\max}=-1.0$ (Beason and Morgan 1984).

This relationship between the normal principle stresses and the probability of failure for a 1 m^2 glass plate is plotted in Fig. 9.

The summation of all the stresses present on the glass surface may be conservatively taken as the maximum applied stress σ_a over the whole plate surface. This is usually overly conservative and a more accurate approach is to summate the contributions of various stressed areas on the surface of the glass to the probability of failure. This approach may be derived from the original formulations of Beason and Morgan (1984) and the elaborations in the draft European Standard (CEN 1997), Overend et al. (1999), and Overend (2002) such that

$$\sigma_p = \left[\frac{1}{A} \int_{\text{area}} (c_b \sigma_{\max})^m \, dA \right]^{1/m} \tag{12}$$

where σ_p=equivalent uniform stress and represents a weighted average of the surface tensile stress distribution on the glass plate. This equation is very convenient because it transforms the actual and complex stress distribution on the glass surface to a single equivalent stress.

Structural Adequacy and Design

The effective uniformly applied stress σ_p derived from Eq. (12) may be finally compared to the failure strength σ_f from Eq. (10) to ensure that

$$\sigma_f \geqslant \sigma_p \tag{13}$$

The accuracy of this method clearly depends on the ability to execute Eq. (12) i.e., to subdivide the glass surface into areas of equal stress, and to subsequently summate the contribution of these areas. This procedure makes the proposed design method unattractive for manual computation. A computer algorithm was therefore developed to determine the equivalent uniform stress σ_p automatically.

The algorithm is written in Visual Basic computer language and makes use of the results obtained from LUSAS, a commercially available finite-element (FE) analysis software (FEA 1999). Input to the algorithm consists of the coordinates of the surfaces to be analyzed and the magnitude of the surface precompression due to the tempering process. The algorithm may be used with a number of commonly used elements ranging from three-noded triangular elements to 20-noded brick elements and conveniently calculates the surface areas, *dA*, and averaged principal tensile stress, $\sigma_{\max}$, for each element of the FE model. All the elements subjected to a compressive stress are eliminated from this summation. The algorithm uses this data to automatically compute the equivalent uniform stress, σ_p, for the whole surface from Eq. (11). The algorithm also creates a spreadsheet containing a listing of these calculations and a summary of the results for the entire surface.

Verification of Failure Models

Experimental investigations were undertaken to verify the accuracy of the proposed failure model and to compare it to the failure predictions obtained from existing failure models. The experimental investigations consisted of undertaking a series of:

1. Ring-on-ring (co-axial ring) tests.
2. Laterally loaded, simply supported plate tests.

These two setups were selected as they provide diverse stress distributions ranging from relatively concentrated stresses in the

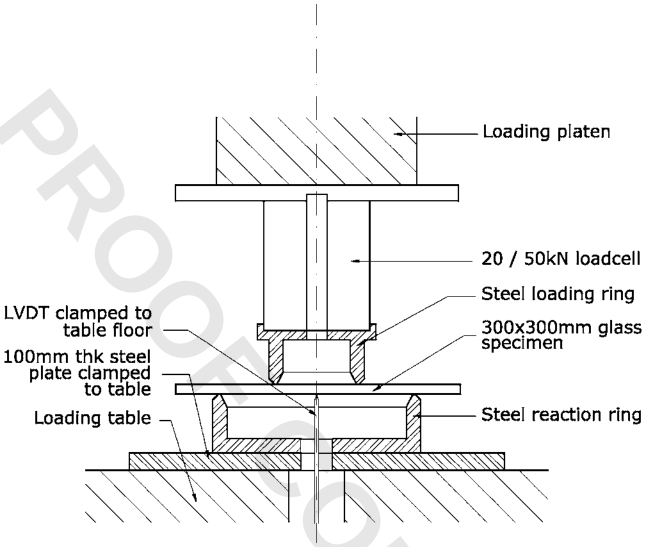

Fig. 10. Ring-on-ring test setup

ring-on-ring tests, to the shallow-gradient stresses that are typical of simply supported plates subjected to uniform lateral loading.

Ring-on-Ring Investigations

A series of ring-on-ring tests were carried out by the writers on as-received glass specimens measuring $300 \times 300 \times 6$ mm thick. The tests were performed by placing the glass plate on a circular steel reaction ring and applying on its opposite surface a load transmitted through a steel loading ring, until failure occurs (Fig. 10). The purpose of this test is to achieve a uniform tensile stress field that is independent of edge effects.

In all 49 ring-on-ring tests were successfully performed. These were composed of 30 annealed glass specimens and 19 tempered glass specimens to BS 6206 class A (BSI 1981) and tested by means of a 51-mm-diameter steel loading ring and one of three different steel reaction rings with 65, 127, and 200 mm diameters (Fig. 10).

Geometrically nonlinear finite-element analysis of the ring-on-ring specimens was undertaken to provide an accurate representation of the surface stresses for the expected large deflections. The maximum surface stresses and maximum deflections obtained from the finite-element analyses were within ±3% of those obtained from the experimental investigation. Furthermore, the FE analysis confirmed that the stress concentrations beneath the loading ring were within ±2% of the stress at midspan. Surface stresses obtained from the finite-element analysis were transformed to an equivalent uniform failure stress and an associated probability of failure by the afore-mentioned computer algorithm. Furthermore, since most failures occurred within the loading ring area, a biaxial stress correction factor $c_b = 1$ was used in Eq. (12).

The probability distribution functions obtained from the proposed GCGM and computer algorithm shows good agreement with the annealed and tempered glass ring-on-ring test data at mean and low probabilities of failure (±4% for both $P_f = 0.5$ and $P_f = 0.1$). However, the predictions for high probabilities of failure are less accurate particularly for the tempered glass where the variation at $P_f = 0.9$ is greater than 12%. (Fig. 11). The increasing inaccuracy with increasing probability of failure for both annealed and tempered glass specimens cannot be fully explained, however the more pronounced variability witnessed in the

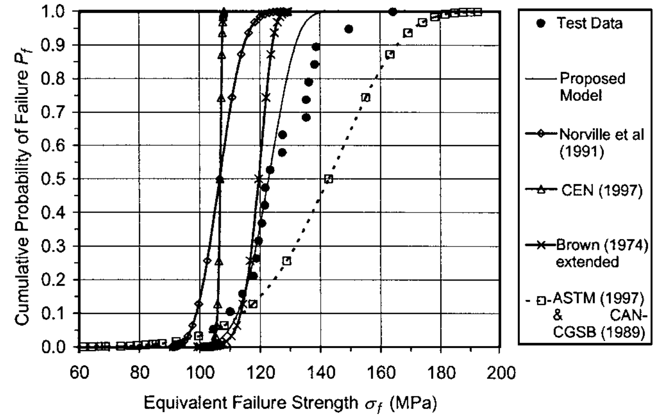

Fig. 11. Test results and failure models for ring-on-ring tempered glass (dotted lines represent weathered glass)

strength of the tempered glass specimens may be attributed to the additional variations caused by the tempering process.

Laterally Loaded Plate Investigations

Two sets of published annealed glass failure data (Beason 1980; Dalgliesh and Taylor 1990) and one set of published failure data for tempered glass (Norville et al. 1991) were used to compare the performance of the existing and the proposed failure models and to further test the validity of the proposed GCGM together with the computer algorithm.

Convergence testing of the FE model ensured that the predicted stresses and deflections were within ±1% of those reported from the experimental investigations.

The computer algorithm was used to summate the major principal surface stresses obtained from each load increment of the FE analysis. The surface precompression σ_r was set to zero for the annealed glass specimens and to 69 $\mathrm{N/mm^2}$ for the tempered glass specimens. This value corresponds to the surface stress measurements carried out by Norville et al. (1991) and agrees with the minimum required value specified in ASTM E-1300 (ASTM 1997). The resulting equivalent uniform stress, σ_p, obtained from the algorithm, was used to determine the probability of failure P_f at every load increment by using Eq. (2).

The relationships between the uniformly distributed, 60 s equivalent load P_{60} and the probability of failure P_f were plotted in Figs. 12 and 13. Fig. 12 shows the probability of failure versus

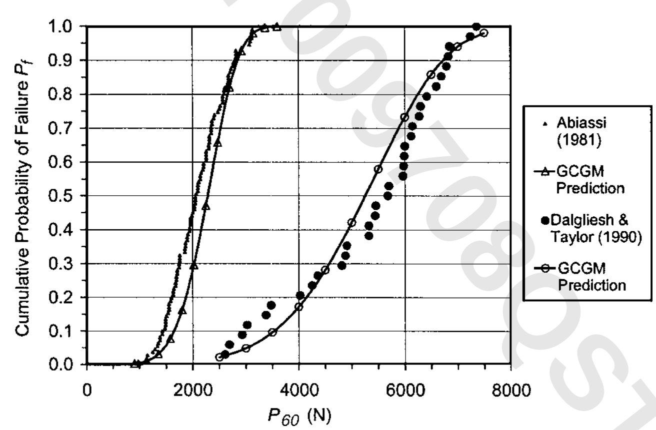

Fig. 12. Test results and GCGM predictions for annealed glass

the 60 s failure load of the published test results (Beason 1980; Dalgliesh and Taylor 1990) and the corresponding GCGM predictions for uniformly loaded, simply supported rectangular annealed glass. Fig. 13 shows the probability of failure versus the 60 s failure load of the published test results (Norville et al.1991) and the corresponding GCGM predictions for uniformly loaded, simply supported rectangular tempered glass.

The predicted relationship between the 60 s equivalent loads, P_{60}, and the probability of failure P_f (Fig. 13) are in good agreement with the annealed and tempered glass test results. Table 3 provides a quantitative comparison of the proposed GCGM at the low probabilities of failure generally used in glass design practice. This table also indicates how the GCGM compares with other failure prediction models at low probabilities of failure. All probabilities of failure in this table have been computed by using the respective surface strength parameters m and k from Table 2.

From Table 3 it is evident that all failure prediction models provide a more accurate, albeit sometimes unsafe, representation of glass strength when compared to the results obtained from the simpler maximum stress approach. The GCGM appears to predict the probability of failure more closely than the other models for both the Dagliesh and Taylor annealed glass (Dagliesh and Taylor 1990) and the Norville et al. tempered glass (Norville et al. 1991). The ASTM E-1300 model provides the best predictions of Beason annealed glass tests (Beason 1980). However, it is important to note that the ASTM E-1300 was partially derived from the Beason (1980) tests. The draft European Standard (CEN 1997), derived from the Sedlacek et al. (1995) model, adopts an uncharacteristically high surface strength parameter, m, and a low parameter k. This in effect restricts its use to very low probabilities of failure ($<8/1{,}000$) as observed in the preceding sections of this paper. This may partly explain the poor predictions at relatively high probabilities of failure shown in Table 3.

Conclusions

A number of existing glass failure models that are used in glass design are reviewed, and the discrepancies between these models, particularly the interpretation of load duration, surface area, and stress distribution, have been identified. Substantial differences have been noted in the magnitude of surface strength parameters and in the effects of the relative magnitude of major and minor principal stress acting on the surface of the glass. These variations

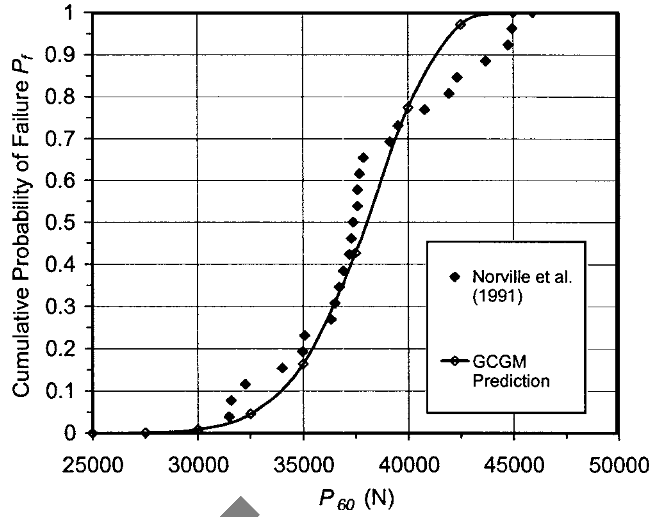

Fig. 13. Test results and GCGM predictions for tempered glass

are shown to translate into considerable differences in the probabilities of failure obtained from the respective models.

A GCGM is proposed by extending the formulations of Fischer-Cripps and Collins (1995). The GCGM combines statistical theory with linear elastic fracture mechanics and allows the surface tensile strength of both annealed and tempered glass to be determined graphically. Furthermore, since the proposed and existing failure models are unattractive for manual computation, a computer algorithm is also put forward. This algorithm calculates the equivalent uniform stress automatically from the results of the finite-element analysis performed on the glass element. The predictions obtained by applying the proposed GCGM are in good agreement with the strength values obtained from ring-on-ring experimental investigations carried out by the writers and experimental investigations on laterally loaded rectangular glass plates carried out by other researchers. Furthermore the use of the computer algorithm resulted in a substantial reduction in computation time.

Further validation of the proposed GCGM and design methodology is required before it can be used by the general engineering community. This includes fundamental research on the nature of flaws in glass and the mechanics of glass failure that will serve to verify the constants such as the stress intensity factor and the

Table 3. Comparison of Reported Test Results and Predicted Probability of Failure

		Probability of failure				
Source	Arbitrary load (kN)	Reported	Predicted from proposed GCGM[a]	Predicted from ASTM & CAN/CGSB[b]	Predicted from CEN[c]	Predicted using maximum stress
Annealed glass Beason (1980)	1.125	0.018	0.010	0.015	0.00026	0.087
Annealed glass Dalgliesh and Taylor (1990)	2.600	0.026	0.025	0.039	0.001	0.094
Tempered glass Norville et al. (1991)	31.500	0.039	0.031	0.001	0.053	1.000

[a]Probability of failure calculated using FE analysis and the computer algorithm with Fischer-Cripps and Collins (1995) surface strength parameters from Table 2.

[b]Probability of failure calculated using FE analysis and computer algorithm with the ASTM (1997) and CAN/CGSB (1989) surface strength parameters shown in Table 2.

[c]Probability of failure calculated using FE analysis and computer algorithm with the CEN (1997) surface strength parameters shown in Table 2.

stress corrosion limit in glass; a full reliability analysis of the test data used to calibrate the United States and European standards in order to verify the surface strength parameters, and the extension of the GCGM to buckling instability and impact loads.

Current and planned research at the University of Nottingham in collaboration with other research institution in the United Kingdom and in Europe includes the application of the GCGM to plates in compression and to built-up glass elements; the testing of a series of 40-year old weathered glass specimens; the use of the GCGM to optimize bolted and adhesive connections in glass; and investigations on the postbreakage performance of safety glass. The results from these research projects will seek to verify the proposed GCGM design methodology to a wider range of structural glass elements.

Notation

The following symbols are used in this paper:

A = surface area;
A_o = datum surface area (=1 m^2);
c = flaw length;
c_b = biaxial stress correction factor;
D = material fracture constant;
h = plate thickness;
K_I = stress intensity factor for mode I loading;
K_{IC} = critical stress intensity factor for mode I loading (plane strain fracture toughness);
k = surface strength parameter;
k_{mod} = stress corrosion ratio;
m = surface strength parameter, Fourier series numerical factor;
n = static fatigue constant;
P_f = probability of failure;
P_{60} = 60 second equivalent failure load;
t_f = load duration;
Y = shape factor;
γ_v = material safety factor for tempered glass;
σ = general applied stress;
σ_a = stress applied perpendicular to crack;
σ_e = 60 s equivalent failure stress;
σ_f = surface tensile strength of glass;
$\sigma_{\max}$ = major principal stress;
$\sigma_{\min}$ = minor principal stress;
σ_p = equivalent uniform stress;
σ_r = surface precompression due to tempering process; and
σ_s = instantaneous failure stress.

References

Abiassi, J. J. (1981). *The strength of weathered window glass using surface characteristics*, Institute for Disaster Research, Texas Tech University Press, Lubbock, Tex.

ASTM. (1997). “Determining load resistance of glass in buildings.” *E 1300–97*, Philadelphia.

Atkins, A. G., and Mai, Y. W. (1988). *Elastic and plastic fracture*, Ellis Horwood Ltd., UK.

Beason, W. L. (1980). *A failure prediction model for window glass*, Institute for Disaster Research, Texas Tech University Press, Lubbock, Tex.

Beason, W. L., and Morgan, J. R. (1984). “Glass failure prediction model.” *J. Struct. Div.*, 110(2), 197–212.

Behr, R. A., Karson, M. J., and Minor, J. E. (1991). “Reliability analysis of window glass failure pressure data.” *Struct. Safety*, 11, 43–58.

British Standards Institute (BSI). (1981). “Impact performance requirements for flat safety glass and safety plastics for use in buildings.” *BS 6206*, UK.

Brown, W. G. (1974). “A practicable formulation for the strength of glass and its special application to large plates.” *Publication No. NRC 14372*, National Research Council of Canada, Ottawa.

Button, D., and Pye, B., eds., (1993). *Glass in building*, Butterworth Architecture, London.

Canadian General Standards Board, (CAN/CGSB). (1989). “Structural design of glass for buildings.” *12.20.M89*, National Standard of Canada, Canada.

Charles, R. J. (1958). “Static fatigue of glass 1&2.” *J. Appl. Phys.*, 29(11), 1549–1560.

Creyke, W., Sainsbury, I., and Morrell, R. (1982). *Design with non-ductile materials*, Applied Science, London.

Dalgliesh, W. A. and Taylor, D. A. (1990). “The strength and testing of window glass.” *Can. J. Civ. Eng.*, 17, 752–762.

European Committee for Standardisation (CEN). (1997). “Glass in building—Design of glass panes—Part 1: General basis of design.” *prEN13474*, Draft European Standard, Brussels, Belgium.

FEA Ltd. (1999). *LUSAS theory manual for LUSAS v13*, Surrey, UK.

Fischer-Cripps, A. C. and Collins, R. E. (1995). “Architectural glazing: Design standards and failure models.” *Build. Environ.*, 30(1), 29–40.

Griffith, A. A. (1920). “The phenomena of rupture and flow of solids.” *Theoretical Transactions of the Royal Society of London*, 221, 163–179.

Holloway, D. G. (1973). *The physical properties of glass*, Wykeham, London.

Inglis, C. E. (1913). “Stresses in a plate due to the presence of cracks and sharp corners.” *Trans. Inst. Naval Archit.*, 55, 219.

Institution of Structural Engineers. (2000). *Structural use of glass in buildings*, London.

Laufs, W., and Sedlacek, G. (1999). “Stress distribution in thermally tempered glass panes near the edges, corners and holes; Part 2. Distribution of thermal stresses.” *Glass Sci. and Technol.*, 72 (2), 42–48.

Lawn, B. R. (1993). *Fracture of brittle solids*, 2nd Ed., Cambridge University Press, Cambridge, UK.

Michalske, T. A. (1983). *Fracture mechanics of ceramics*, R. C. Bradt, A. G. Evans, D. P. H. Hasseleman, and F. F. Lange, eds., Vol. 5, Plenum, New York.

Norville, H. S., Bove, P. M. and Sheridan, D. L. (1991). *The strength of new thermally tempered window glass lites*, Glass Research and Testing Lab, Texas Tech University, Lubbock, Texas.

Overend, M. (2002). “The appraisal of structural glass assemblies.” Ph.D. thesis, Univ. of Surrey, Surrey, UK.

Overend, M., Buhagiar, D., and Parke, G. A. R. (1999). “Failure prediction-What is the true strength of glass?” *Proc., Glass in Buildings*, Univ. of Bath, Bath, UK.

Porter, M. I. and Houlsby, G. T. (2001). “Development of crack size limit state design methods for edge-abraded glass members.” *Struct. Eng.*, 79(8), 29–35.

Sedlacek, G., Blank, K., and Gusgen, J. (1995). “Glass in structural engineering.” *Struct. Eng.*, 73(2), 17–22.

Shand, E. B. (1961). “Correlation of strength of glass with fracture flaws of measured size.” *J. Am. Ceram. Soc.*, 44(9), 451–455.

Shand, E. B. (1965). “Strength of glass—The Griffith method revised.” *J. Am. Ceram. Soc.*, 48(1), 43–49.

Wan, K. T., Lathabai, S., and Lawn, B. R. (1961). “Crack velocity functions and thresholds in brittle solids.” *J. Am. Ceram. Soc.*, 44, 21–26.

Weibull, W. (1951). “A statistical distribution function of wide applicability.” *J. Appl. Mech.*, 18, 293–297.

Wiederhorn, S. M. (1977). “Dependence of lifetime predictions on the form of the crack propagation equation.” *Fracture ICF4*, 893–901.

Wiederhorn, S. M. and Bolz, L. H. (1970). “Stress corrosion and static fatigue of glass.” *J. Am. Ceram. Soc.*, 53(10), 543–548.